Available online at www.sciencedirect.com
ScienceDirect
Ceramics International 38 (2012) 351–356
CERAMICS INTERNATIONAL
www.elsevier.com/locate/ceramint

Densification, microstructure and mechanical properties of SiO_2–cBN composites by spark plasma sintering

Jianfeng Zhang, Rong Tu *, Takashi Goto

Institute for Materials Research, Tohoku University, Sendai 980-8577, Japan

Received 28 April 2011; received in revised form 1 July 2011; accepted 5 July 2011
Available online 18th July 2011

Abstract

SiO_2–cBN composites were consolidated by spark plasma sintering at 1473–1973 K. The effects of cBN content and sintering temperature on the relative density, phase transformation, microstructure and mechanical properties of the SiO_2–cBN composites were investigated. The relative density of the SiO_2–cBN composites increased with increasing SiO_2 content. The phase transformation of cBN to hBN in SiO_2–cBN composites was identified at 1973 K, showing the highest transformation temperature in cBN-containing composites. The SiO_2–20 vol% cBN composites sintered at 1673 K showed the highest hardness and fracture toughness of 12.5 GPa and 1.5 MPa $m^{1/2}$, respectively.

Keywords: C. Mechanical properties; Cubic boron nitride; Silicon oxide; Spark plasma sintering; Phase transformation

1. Introduction

Since SiO_2 has excellent electrical-insulation, high chemical stability, a low thermal expansion coefficient and low thermal conductivity [1–3], it has been applied as a refractory material in crucibles for melting high-purity silicon and in circuit boards. However, the low hardness and high brittleness limits its applications as a structural material. The fabrication of SiO_2-based composites with a hard phase is a promising way to improve the hardness and fracture toughness of SiO_2.

Like SiO_2, cubic boron nitride (cBN) has low thermal expansion and electrical conductivity [4,5], but unlike SiO_2, it is characterized by the high hardness and thermal conductivity [5–7]. Although cBN is hardly densified, SiO_2 is easily densified by hot pressing. Since cBN does not readily react with SiO_2, SiO_2–cBN composite should be a promising structural material. However, no report on SiO_2–cBN composite has been published to date.

Spark plasma sintering (SPS) has been widely used for the densification of materials due to its rapid heating, low sintering temperature and short sintering time. To date, many kinds of fully dense high-temperature structural ceramics [8,9], transparent ceramics [10,11], and intermetallics [12] have been successfully fabricated. SPS would inhibit the phase transformation of cBN to hBN due to the short sintering time. In the present study, SiO_2–cBN composites were prepared by SPS and the effects of cBN content and sintering temperature on the density, micorstructure and mechanical properties of SiO_2–cBN composites were investigated.

2. Experimental details

SiO_2 (SO-E1, Admatechs, mean diameter: 0.25 μm) and cBN (SBN-F, Showa Denko, mean diameter: 2.8 μm) powders were used as raw materials. cBN at 0–50 vol% was mixed with SiO_2 by a planetary ball mill at a rotary rate of 120 rpm for 48 h in ethanol. The mixed powder was dried at 333 K for 24 h and then passed through a 100-μm sieve three times. The powder was poured into a graphite die with an inner diameter of 10 mm and sintered by SPS (SPS-210LX, SPS Syntex Inc, Japan) at 1473–1973 K at a heating rate of 1.67 K s^{-1}, a holding time of 0.6 ks and a pressure of 100 MPa. The temperature was measured by an optical pyrometer focused on a hole (Ø 2 mm × 5 mm) in the graphite die. The shrinkage of the specimens was continuously monitored by the displacement of a punch rod. The shrinkage was calibrated by deducting the displacement of the graphite die.

* Corresponding author. Tel.: +81 22 215 2106.
E-mail address: turong@imr.tohoku.ac.jp (R. Tu).

0272-8842/$36.00
doi:10.1016/j.ceramint.2011.07.013

The phase transformation of cBN was examined by X-ray diffraction (XRD; Geigerflex, Rigaku Corp.) with CuKα radiation. The microstructures of the polished and fracture surfaces were observed by scanning electron microscopy (SEM, Hitachi: S-3100H). The density of the specimens was determined by the Archimedes' method, and the relative density (D_r) was calculated using theoretical densities of SiO_2 (2.20×10^3 kg m^{-3}) [13] and cBN (3.49×10^3 kg m^{-3}) [14]. Vickers hardness (H_v/GPa) and fracture toughness (K_{IC}/MPa m$^{1/2}$) at room temperature were measured using a micro-hardness tester (HM-221, Mitutoyo) at loads of 0.98 and 9.8 N. The hardness was calculated using Eq. (1):

$$H_v = 1.854 \times 10^{-9} \times \frac{P}{d^2} \quad (1)$$

where P (N) is the applied load and d (m) is the average value of the two diagonal lengths for Vickers indentation. The K_{IC} (MPa m$^{1/2}$) was calculated from Eq. (2) using the half length of the crack (c, m) formed around the corners of indentations [15,16]:

$$K_{IC} = 0.073 \times 10^{-6} \times \frac{P}{c^{3/2}} \quad (2)$$

where P (N) is the applied load and c (m) is the average half length of cracks.

3. Results and discussion

Fig. 1 shows the effect of sintering temperature on shrinkage from 1273 to 1673 K and the isothermal shrinkage at 1673 K for 0.6 ks for SiO_2–cBN composites with cBN content (C_{cBN}) from 0 to 50 vol%. The shrinkage of monolithic SiO_2 started at 1273 K and finished at 1573 K. The SiO_2–cBN composites at C_{cBN} = 10, 20 and 30 vol% started to shrink at 1473 K and ceased shrinking at 1623 K. On the other hand, the shrinkage of

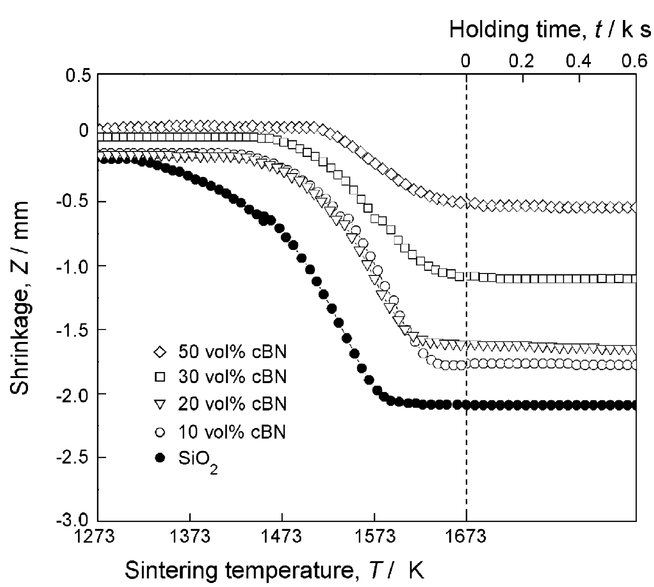

Fig. 1. Effect of sintering temperature on the displacement of SiO_2 and SiO_2–cBN composites originally containing 10–50 vol% cBN at 1473–1673 K, and the time dependence of isothermal displacement at 1673 K up to 0.6 ks. The height of each green sample was 5 mm.

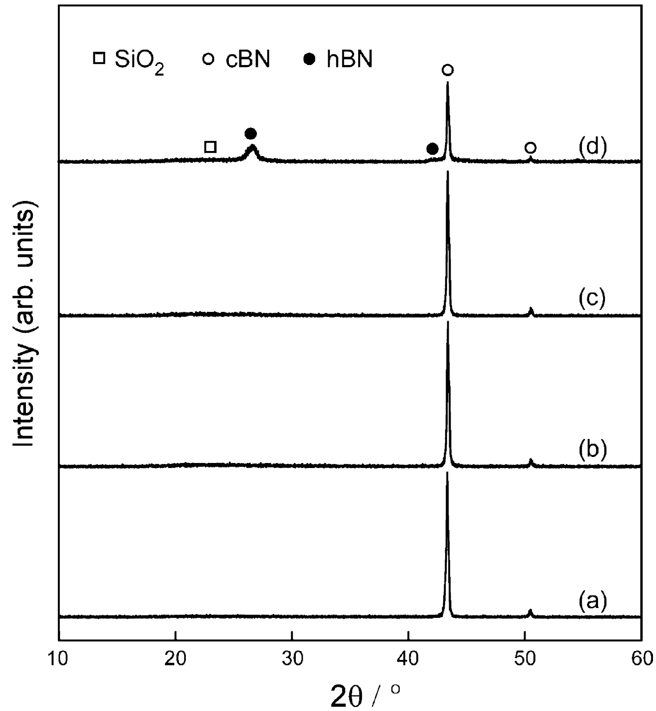

Fig. 2. XRD patterns of SiO_2–cBN composites originally containing 50 vol% cBN sintered at (a) 1573, (b) 1673, (c) 1873 and (d) 1973 K.

SiO_2–50 vol% cBN composite started at 1523 K and continued even in the soaking period at 1673 K.

Fig. 2 shows the XRD patterns of SiO_2–50 vol% cBN composites sintered at 1573–1973 K. SiO_2 was still amorphous after sintering at 1573–1973 K. No phase transformation of cBN to hBN was observed at 1873 K, whereas a small amount of hBN was identified at 1973 K. SiO_2 had no reaction with cBN in the whole temperature range. Fig. 3 demonstrates the starting temperature of the phase transformation of cBN to hBN (T_{cBN}) in cBN-containing composites. In Al_2O_3–Ni–cBN [17],

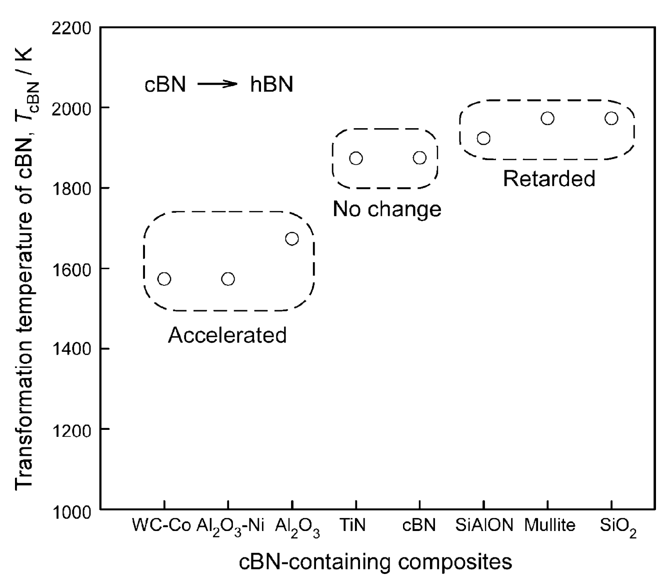

Fig. 3. Starting temperature of the phase transformation of cBN to hBN in different cBN-containing composites and cBN.

WC–Co–cBN [18] and Al_2O_3–cBN composites [19], cBN transformed to hBN at 1573–1673 K. Thus, the other phases, i.e., WC–Co, Al_2O_3–Ni and Ni, could accelerate the transformation. The T_{cBN} in TiN–cBN [20] was the same as that of cBN. In SiAlON–cBN [6,21], mullite–cBN [7] and SiO_2–cBN systems, the T_{cBN} was 1923–1973 K, 50–100 K higher than that of cBN. This indicates that SiO_2-containing phases were effective for retarding the phase transformation.

Fig. 4 shows the effect of C_{cBN} on the relative density (D_r) of SiO_2–cBN composite sintered at 1473–1873 K. The effect of C_{cBN} on the D_r of TiN–cBN [20] and mullite–cBN [7] at 1873 K is also presented in this figure for comparison. At 1473 K, the D_r of SiO_2 was 98.7%. With increasing C_{cBN} from 10 to 50 vol%, the D_r of SiO_2–cBN composites decreased from 97.9% to 88.3%. At 1573 K, the D_r of SiO_2–(10–20) vol% cBN composites was higher than 99%. With increasing C_{cBN} from 30 to 50 vol%, the D_r of SiO_2–cBN composites decreased from 97.1% to 90.6%. At 1673 K, the D_r of SiO_2–(10–20) vol% cBN composites was almost the same as that at 1573 K, whereas the D_r of SiO_2–30 vol% cBN and 50 vol% cBN was 98.0% and 92.4%, higher than that at 1573 K. At 1773 K, the SiO_2–cBN composites at C_{cBN} = 0–20 vol% did not consolidate because the graphite die was broke. At 1773 and 1873 K, the D_r of SiO_2–50 vol% cBN was 91% and 90%, respectively, lower than that at 1673 K. The higher temperature hindered the densification due to the transformation. The D_r of the SiO_2–cBN composites at 1573 K and C_{cBN} = 10–20 vol% (above 99%) was higher than that of TiN–cBN (92–93%) and mullite–cBN (96–98%) composites at 1873 K and C_{cBN} = 10–20 vol%.

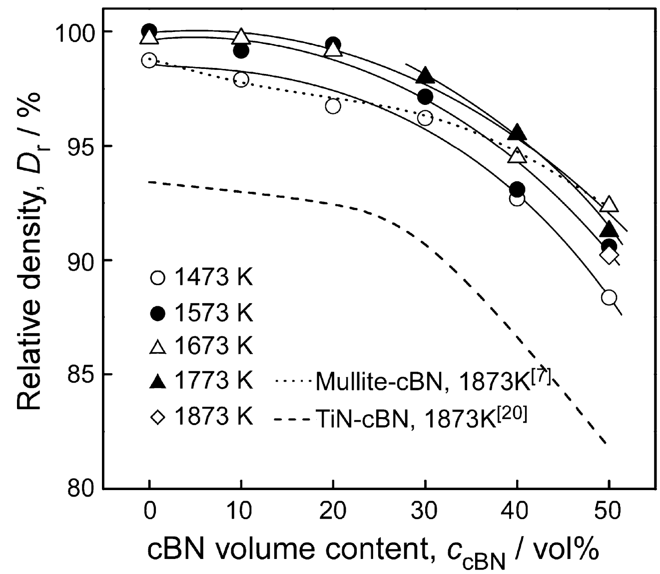

Fig. 4. Effect of cBN content on the relative density of SiO_2–cBN composites sintered at 1473–1873 K.

Fig. 5 shows the back-scattered electron images of SiO_2–cBN composites containing 10–50 vol% cBN sintered at

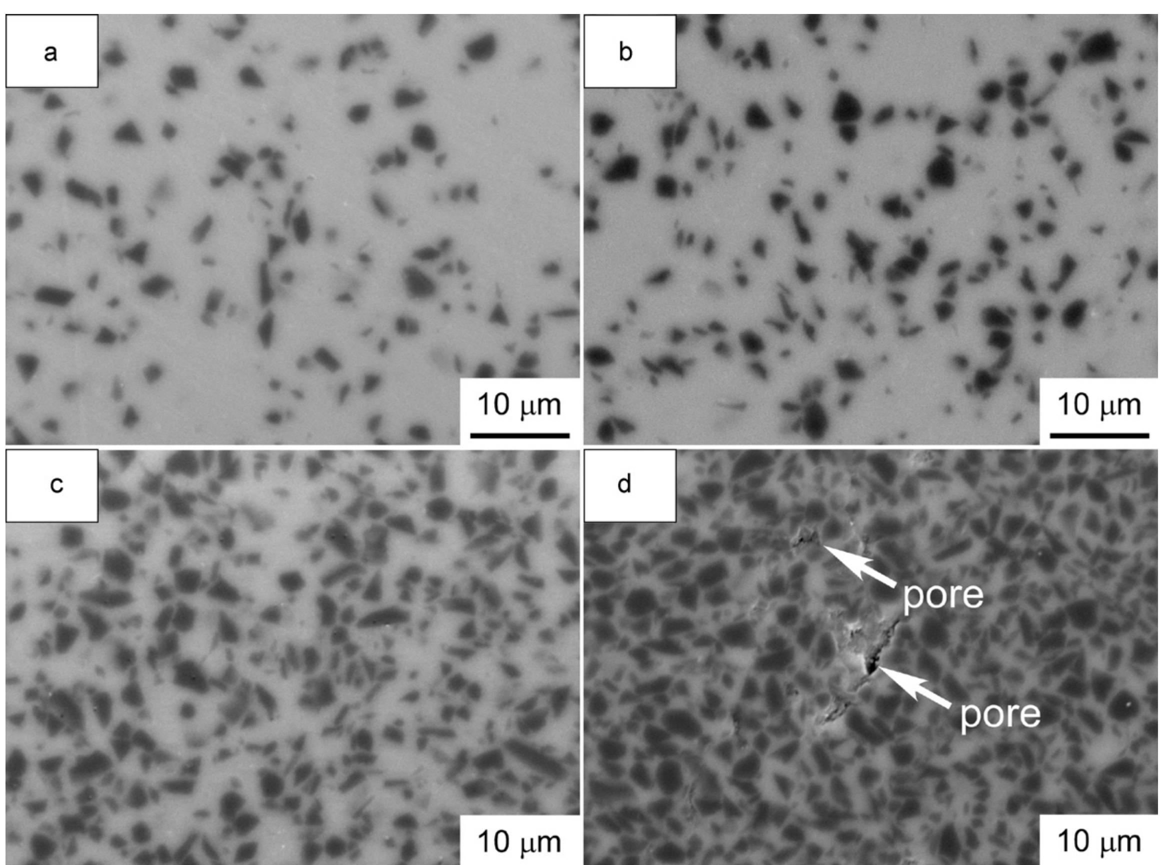

Fig. 5. Back-scattered SEM micrographs of the polished surface of SiO_2–cBN composites originally containing (a) 10, (b) 20, (c) 30 and (d) 50 vol% cBN sintered at 1673 K.

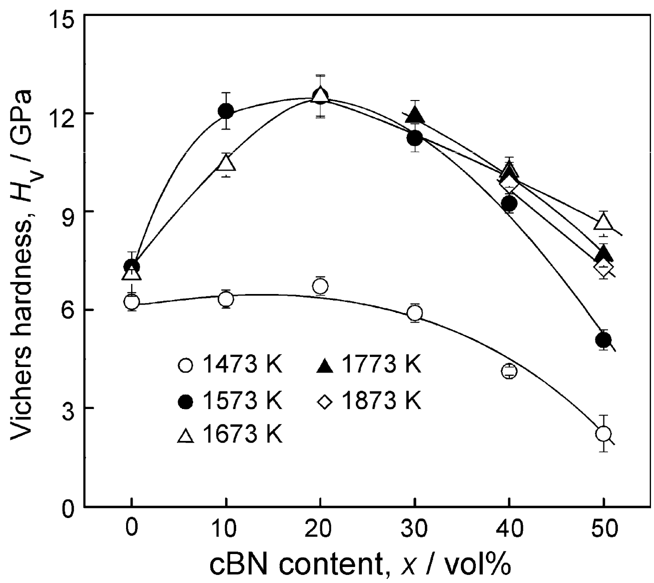

Fig. 6. Effect of cBN content on the Vickers hardness of SiO_2–cBN composites sintered from 1473 to 1873 K.

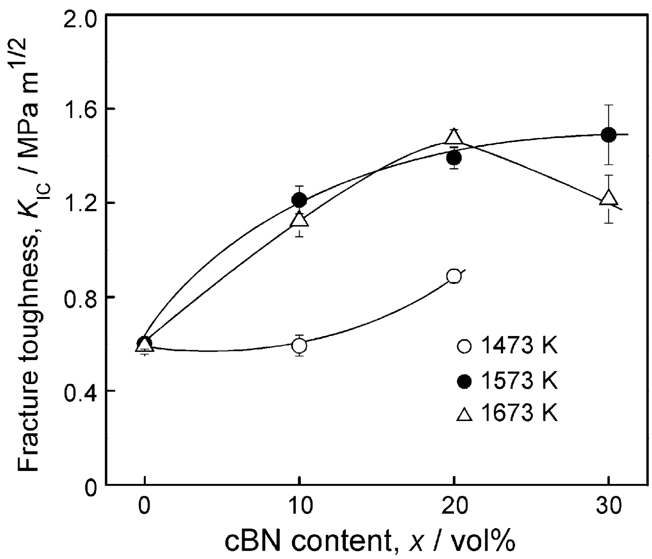

Fig. 7. Effect of cBN content on the fracture toughness of SiO_2–cBN composites sintered from 1473 to 1673 K.

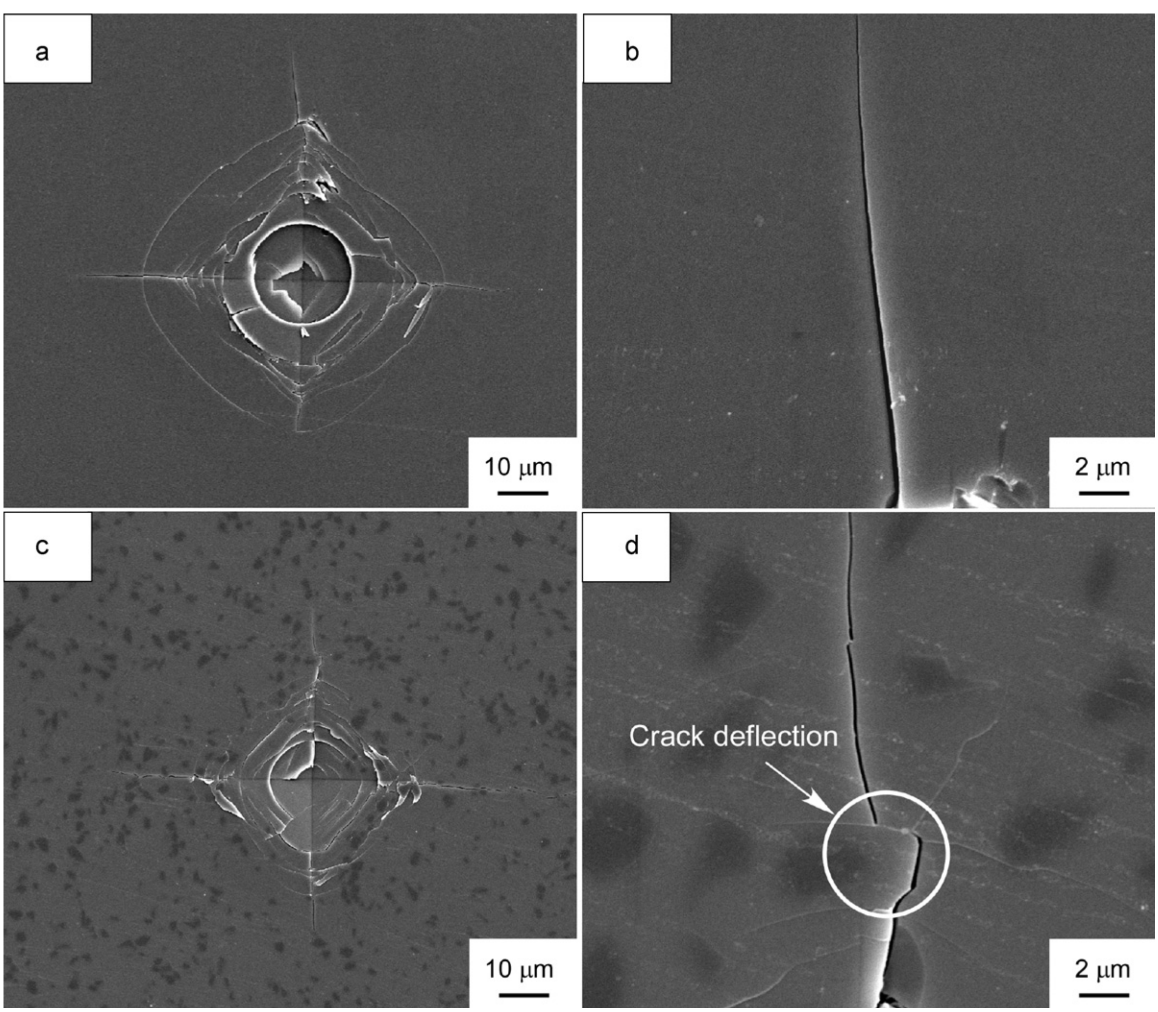

Fig. 8. SEM image of the typical crack propagation in SiO_2 ((a) and (b)) and SiO_2–20 vol% cBN composite ((c) and (d)).

1673 K. The black phase is cBN and the white matrix is SiO_2. No pores were identified in the SiO_2–cBN composites containing 10–30 vol% cBN (Fig. 5(a)–(c)). However, some pores and cracks were observed in SiO_2–50 vol% cBN composite.

Fig. 6 shows the effect of C_{cBN} on H_v of the SiO_2–cBN composites sintered at 1473–1873 K. The H_v of SiO_2 was 6.2 GPa at 1473 K and increased slightly to 7.0 GPa at 1573 and 1673 K. At 1473 K, the H_v of SiO_2–cBN composites slightly increased to 6.5 GPa with increasing C_{cBN} to 20 vol% and then decreased to 2 GPa at C_{cBN} = 50 vol%. At 1573 K, the H_v increased to 12 GPa with increasing C_{cBN} to 20 vol% and then decreased to 5 GPa at C_{cBN} = 50 vol%. At 1673 K, the H_v showed the maximum of 12.5 GPa at C_{cBN} = 20 vol%. The H_v of the SiO_2–cBN composites at 1773 K decreased from 11.7 to 7.7 GPa with increasing C_{cBN} from 30 to 50 vol%. At 1873 K, the H_v of the SiO_2–cBN composite at C_{cBN} = 50 vol% was 7.3 GPa, 0.4 GPa lower than that at 1773 K and C_{cBN} = 50 vol%.

Fig. 7 shows the effect of C_{cBN} on the K_{IC} of the SiO_2–cBN composites sintered at 1473–1673 K. The K_{IC} of SiO_2 was 0.6 MPa $m^{1/2}$, showing a typical value of glass materials due to their high brittleness [11,22]. The K_{IC} of SiO_2–cBN composites increased with increasing C_{cBN}. At 1473 K, the K_{IC} of SiO_2–20 vol% cBN increased to 0.8 MPa $m^{1/2}$. At 1573 and 1673 K, the highest K_{IC} was 1.5 MPa $m^{1/2}$, 2.5 times higher than that of SiO_2. Fig. 8 shows the indentation and crack propagation in SiO_2 and SiO_2–20 vol% cBN. The indentation in SiO_2 was much bigger than that in SiO_2–20 vol% cBN composite and the center of indentation in SiO_2 was collapsed. The crack in SiO_2 propagated straight in SiO_2 (Fig. 8(a) and(b)); however, the crack was deflected in the SiO_2–20 vol% cBN composite (Fig. 8(c) and (d)). The crack deflection may have contributed to the higher K_{IC} compared with that of SiO_2. It has been reported that cBN improved the K_{IC} of composites, such as α-Al_2O_3–cBN [19], TiN–cBN [7] and WC–Co–cBN [18]. Martinez et al. have reported that the K_{IC} of WC–Co–30 vol% cBN composite had a maximum value of 15.4 MPa $m^{1/2}$, almost 2 times higher than that of WC–5 wt% Co (7.3 MPa $m^{1/2}$) [18]. The maximum K_{IC} of α-Al_2O_3–20 vol% cBN composite at 1573 K was 4.1 MPa $m^{1/2}$, about 1.5 times higher than that of α-Al_2O_3 (2.7 MPa $m^{1/2}$) [19]. In TiN–cBN composites, the K_{IC} of TiN–(10–20) vol% cBN composites sintered at 1873 K was 3.4–3.6 MPa $m^{1/2}$, about 1.1 times higher than that of TiN sintered at 1873 to 2073 K (3.0–3.2 MPa $m^{1/2}$) [7].

4. Conclusions

SiO_2–cBN composites were consolidated by SPS at 1473–1673 K under a moderate pressure of 100 MPa. With increasing cBN content, the starting and finishing temperature of shrinkage of SiO_2–cBN composites increased and the relative density gradually decreased. The phase transformation temperature of cBN to hBN was 1973 K, higher than the other cBN-containing composites. No reaction between SiO_2 and cBN was identified. The relative density of SiO_2–(10–30) vol% cBN composites was about 96–100% at 1473–1673 K. The highest hardness and fracture toughness of SiO_2–20 vol% cBN composites sintered at 1673 K were 12 GPa and 1.5 MPa $m^{1/2}$, respectively.

Acknowledgements

This research was financially supported by the Japan Society for the Promotion of Science (JSPS), Grant-in-Aid for JSPS fellow, 22-00365, Japan, the Rare Metal Substitute Materials Development Project, the New Energy and Industry Technology Development Organization (NEDO), the Global COE Program ‘‘Materials Integration (International Center of Education and Research), Tohoku University’’ and the International Collaboration Center, ICC-IMR, Tohoku University.

References

[1] T. Kokubo, Bioactive glass ceramics: properties and applications, Biomaterials 12 (2) (1991) 155–163.
[2] T. Uchino, Structure and properties of amorphous silica and its related materials: recent developments and future directions, Journal of the Ceramic Society of Japan 113 (1313) (2005) 17–25.
[3] R.K. Brow, M.L. Schmitt, A survey of energy and environmental applications of glass, Journal of the European Ceramic Society 29 (7) (2009) 1193–1201.
[4] R.H. Wentorf, R.C. DeVries, F.P. Bundy, Sintered superhard materials, Science 208 (1980) 873–880.
[5] H.O. Pierson, Handbook of Refractory Carbides and Nitrides, William Andrew Publishing/Noyes, 1996.
[6] M. Hotta, T. Goto, Densification and phase transformation of β-SiAlON–cubic boron nitride composites prepared by spark plasma sintering, Journal of the American Ceramic Society 92 (8) (2009) 1684–1690.
[7] M. Hotta, T. Goto, Densification: phase transformation and hardness of mullite–cubic BN composites prepared by spark plasma sintering, Journal of the Ceramic Society of Japan 118 (1374) (2010) 157–160.
[8] Y. Zhao, et al., Preparation and microstructure of a ZrB_2–SiC composite fabricated by the spark plasma sintering–reactive synthesis (SPS–RS) method, Journal of the American Ceramic Society 90 (12) (2007) 4040–4042.
[9] I. Akin, et al., Microstructure and densification of ZrB_2–SiC composites prepared by spark plasma sintering, Journal of the European Ceramic Society 29 (11) (2009) 2379–2385.
[10] L. An, A. Ito, T. Goto, Highly transparent lutetium titanium oxide produced by spark plasma sintering, Journal of the European Ceramic Society 31 (1–2) (2010) 237–240.
[11] L. Wang, W. Jiang, L. Chen, Z. Shen, Formation of a unique glass by spark plasma sintering of a zeolite, Journal of Materials Research 24 (10) (2009) 3241–3245.
[12] Q. He, C. Jia, J. Meng, Influence of iron powder particle size on the microstructure and properties of Fe_3Al intermetallics prepared by mechanical alloying and spark plasma sintering, Materials Science and Engineering A 428 (1–2) (2006) 314–318.
[13] JCPDS, International Centre for Diffraction Data, No. 27-0605.
[14] JCPDS, International Centre for Diffraction Data, No. 25-1033.
[15] B.R. Lawn, E.R. Fuller, Equilibrium penny-like cracks in indentation fracture, Journal of Materials Science 10 (12) (1975) 2016–2024.
[16] K. Tanaka, Elastic/plastic indentation hardness and indentation fracture toughness: the inclusion core model, Journal of Materials Science 22 (4) (1987) 1501–1508.
[17] J.F. Zhang, R. Tu, T. Goto, Spark plasma sintering of Al_2O_3–cBN composites assisted by precipitating Ni nanoparticle precipitated by rotary chemical vapor deposition, Journal of the European Ceramic Society 31 (12) (2011) 2083–2087.

[18] V. Martínez, J. Echeberria, Hot isostatic pressing of cubic boron nitride–tungsten carbide/cobalt (cBN–WC/Co) composites: effect of cBN particle size and some processing parameters on their microstructure and properties, Journal of the American Ceramic Society 90 (2) (2007) 415–424.
[19] M. Hotta, T. Goto, Densification and microstructure of Al_2O_3–cBN composites prepared by spark plasma sintering, Journal of the Ceramic Society of Japan 116 (1354) (2008) 744–748.
[20] M. Hotta, T. Goto, Spark plasma sintering of TiN–cubic BN composites, Journal of the Ceramic Society of Japan 118 (1374) (2010) 137–140.
[21] M. Hotta, T. Goto, Spark plasma sintering of βSiAlON–cBN composite, Materials Science Forum 561–565 (2007) 599–602.
[22] C.A.R. Costa, L.F. Valadares, F. Galembeck, Stoer silica particle size effect on the hardness and brittleness of silica monoliths, Colloids and Surfaces A: Physicochemical and Engineering Aspects 302 (1–3) (2007) 371–376.